

# Automated Label-Free Imaging Assay for Measuring T Cell Activation and Cluster Formation

## Authors

Paul Held, Peter J. Brescia, and  
Joe Clayton  
Agilent Technologies, Inc.

## Abstract

This application note presents an automated, label-free imaging assay for quantifying T cell and CAR T cell activation through cluster formation. Using brightfield microscopy and Agilent BioTek Gen5 software, the assay enables real-time, kinetic analysis of immune cell clustering in response to CD3/CD28 or antigen stimulation. Results show that cluster formation and area correlate with activation status and are influenced by stimulant concentration. Integration with the Agilent BioTek BioSpa live cell analysis system supports high-throughput, reproducible analysis, offering a flexible and scalable solution for evaluating T cell function in immunotherapy research.

## Introduction

T cells play a critical role in triggering adaptive immune responses by recognition of antigens. Importantly, the adaptive immune response improves with time and results in the generation of immunological memory and long-lasting protection.

In vertebrates, T lymphocytes constantly scan the surface of antigen-presenting cells (APCs) for the detection of foreign peptide fragments bound in the peptide-MHC (pMHC). Recognition takes place via the pMHC binding to T-cell receptors (TCRs) and the transduction of the signal through the downstream signaling cascade. It is essential that T cells be activated when binding to foreign peptides occurs and not when confronted with self-peptides. Failures in the discrimination process result in either infection or autoimmune diseases.<sup>1</sup>

T cell activation requires at least two signals to be fully activated. The first signal is initiated by the TCR interacting with foreign pMHC on an APC. Interaction of CD4/CD8 coreceptors with MHC recruits Lck to the TCR complex, where it phosphorylates and activates Zap70, which provides signal one. Ligation of the costimulatory receptor CD28 by CD80/CD86 results in PI3K activation and delivers signal two for full T cell activation (Figure 1).<sup>2</sup>

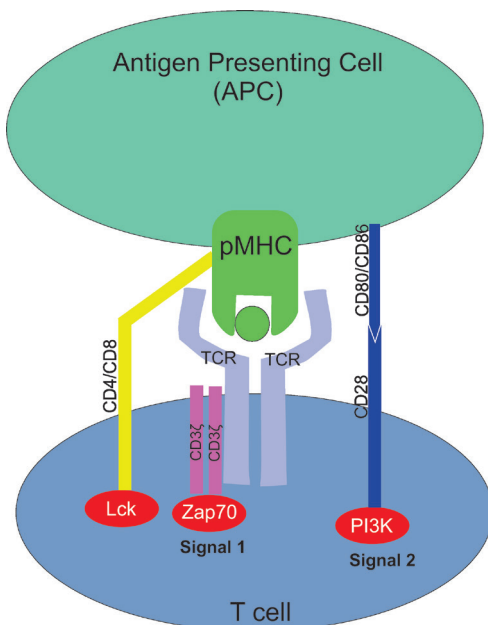


**Figure 1.** T cell activation from interaction with antigen presenting cell.

CAR T cells can be activated by a single tumor antigen. A typical second-generation CAR contains the CD3ζ and CD28 endo-domains in cis. Interaction with a single antigen is sufficient to deliver both signals one and two, resulting in T cell activation (Figure 2).

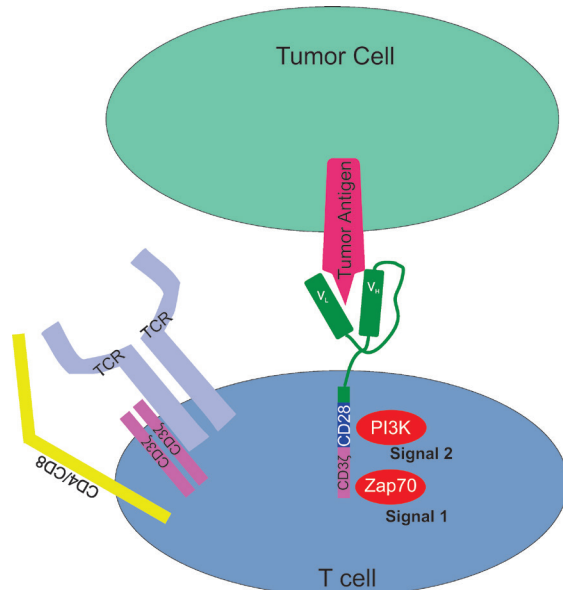


**Figure 2.** CAR T cell activation by cancer cell.

T cell activation induces the upregulation of several cell surface markers that occur in a temporal progression. CD69 and the serum iron-transport protein CD71 are expressed quite rapidly after activation.<sup>4</sup> The CD25 antigen upregulates later in the activation process, upon stimulation of the TCR/CD3 complex, which is considered a hallmark molecular indicator of T cell activation.<sup>5</sup>

## Experimental

T47D-mKate2 cells were cultured in RPMI 1640 (Life Technologies, part number 11875-093) supplemented with 10% fetal bovine serum (FBS), penicillin-streptomycin, and 0.2 U/mL insulin (Sigma Aldrich, part number I-1882) at 37 °C in 5% CO<sub>2</sub>. Cultures were routinely trypsinized (0.05% trypsin-EDTA) at 80% confluence.

For T cell activation experiments, naïve T cells were thawed from liquid nitrogen frozen stocks and allowed to recover overnight. The following day, CAR T cells were seeded into Agilent 96-well microplates, black-sided, clear bottom (part number 204626-100) at 100,000 cells per well in 100 µL of ImmunoCult-XF cell expansion media (StemCell Technologies). Various concentrations of ImmunoCult Human

CD3/CD28 T cell activator (StemCell Technologies) were added to the wells in 100  $\mu$ L as 2x solutions. The cells were imaged every two hours for five days.

For CAR T cell activation experiments, epithelial cell adhesion molecule (EpCAM)-specific CAR T cells were thawed from liquid nitrogen frozen stocks and allowed to recover overnight. The following day, CAR T cells were seeded into Agilent 96-well microplates, black-sided, clear bottom, at 100,000 cells per well in 100  $\mu$ L of ImmunoCult-XF cell expansion media. Activation was carried out by adding a range of EpCAM concentrations to the wells in 100  $\mu$ L as 2x solutions in media. Following the addition of EpCAM, cells were imaged every two hours for five days.

For experiments with mammalian cells, lymphocytes were activated for seven days before their addition. CAR T lymphocytes were stimulated as described above using a final EpCAM concentration of 250  $\mu$ g/mL. Cells were incubated for three days at 37 °C and 5% CO<sub>2</sub> and diluted eight-fold with fresh media. The cells were then rechallenged and incubated for another three days. T47D-mKate2 cells were trypsinized, counted and seeded into Agilent 96-well microplates, black-sided, clear bottom, at 5,000 cells per well in 200  $\mu$ L of media. The following day, dilutions of activated CAR T lymphocytes were added in 100  $\mu$ L of XF cell expansion media before initiating the imaging routine, with images captured every two hours for five days.

### Imaging

Wells were imaged kinetically using either an Agilent BioTek Lionheart FX automated microscope or an Agilent BioTek Cytation 5 cell imaging multimode reader in both the bright-field and TRITC fluorescent channels with a 4x objective. Cells were maintained at 37 °C in a 5% CO<sub>2</sub> environment. Camera exposure settings were set manually with the BioTek Gen5 software auto-exposure routine on control wells prior to imaging the plate. A laser autofocus routine was used for rapid focusing on each well.

### Image analysis

Cell clusters were identified using the cell analysis data reduction feature of Gen5 software, based on the presence of dark spots on a light background in the brightfield channel object intensity and size discrimination. Once identified, clusters were analyzed to determine the quantity, individual cluster size, and total cluster area throughout the kinetic assay.

## Results and discussion

Quantification of T cell clustering following T lymphocyte activation and clustering resulting from the addition of soluble antibody complexes binding to CD3 and CD28 surface ligands can be monitored using brightfield imaging. As shown in Figure 3, activated T cells form clusters that are identified and quantitated using image analysis. The clusters start out as numerous small dark spots that grow and coalesce into fewer, but much larger cell clusters.

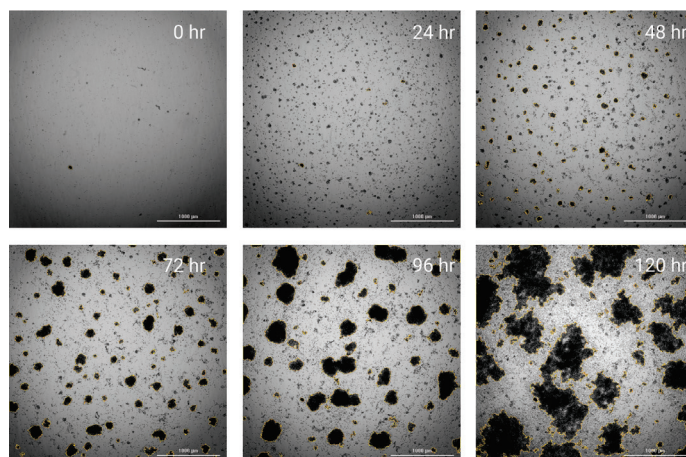


**Figure 3.** Brightfield imaging and analysis supports the quantification of T lymphocyte activation and clustering. Naïve T lymphocytes were incubated with a CD3/CD28 stimulation cocktail. Brightfield images (4x) were captured of the same well every 24 hours for five days. Yellow masking depicts cluster area identified with image analysis.

Varying concentrations of CD3/CD28 T cell activator were incubated with T lymphocytes to characterize the extent and timing of cluster formation. Following the addition of the activation cocktail, the total cluster area increased for approximately five days, after which the cluster area began to decrease. Interestingly, dilutions from the vendor's suggested concentration (1x) appear to be slightly less effective at eliciting T cell clustering than lower concentrations of the CD3/CD28 cocktail, with maximum clustering observed with a 0.125x dilution (Figure 4).

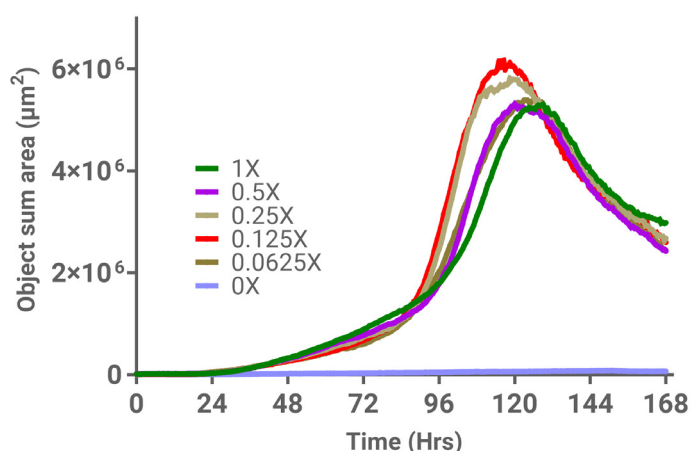


**Figure 4.** Brightfield imaging and analysis supports the quantification of T lymphocytes. The total cluster area of cells activated with various concentrations of CD3/CD28 cocktail. T lymphocytes were exposed to various concentrations of CD3/CD28 activation cocktail. Brightfield images were captured every 0.5 hours for seven days. Image analysis was used to calculate total cluster area at each time point. Data represents the mean and standard deviation of eight determinations.

When the total cluster area for different concentrations of the CD3/CD28 cocktail are plotted after a five-day exposure period, the maximal spot area was achieved with about 10% of the vendor recommended dosage (Figure 5). Further dilution resulted in markedly less clusters, while an increase in dosage had only a marginal effect. This suggests that a minimal concentration of CD3 and CD28 are necessary to activate a given number of T cells.

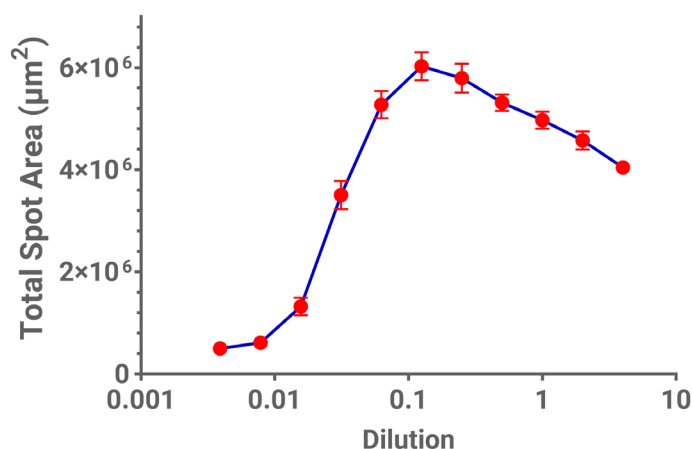


**Figure 5.** Total T cell cluster area for various dilutions of CD3/CD28 mixture. The total T lymphocyte cluster area was calculated for each well after 120 hours of exposure to various dilutions of a CD3/CD28 mixture. Data represents the mean and standard deviation of eight determinations.

Kinetic analysis of several dilutions of the cocktail demonstrates a sigmoidal curve. As seen in Figure 6, dilutions of the mixture above 0.1 result in a similar response. Further dilution of the CD3/CD28 mixture resulted in less cluster formation.

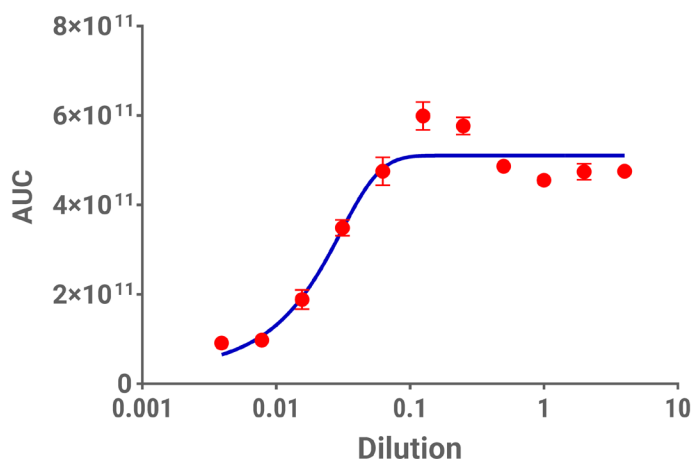


**Figure 6.** Relationship of cluster area and CD3/CD28 dilution. T cells were exposed to various dilutions of CD3/CD28 and brightfield images were captured every 0.5 hours for five days. Using kinetic analysis, the total cluster area is plotted as a function of time. The subsequent AUC for each dilution is calculated and plotted as a function of EpCAM concentration. Data represents the mean and standard deviation of eight determinations.

### Quantification of CAR T cell activation and clustering following exposure to target antigen

CAR T cells can be activated in a similar manner to normal T cell lymphocytes by exposing them to their engineered target antigen in solution. For this study, CAR T cells targeting EpCAM were exposed to varying concentrations of EpCAM protein added to the growth medium and monitored via automated imaging, as described previously. CAR T cells exposed to EpCAM result in a pronounced increase in total cluster area over five days, while naïve T cells exhibit only a slight increase in cluster formation (Figure 7). In both cases, 100,000 cells were seeded into wells in the presence of 1  $\mu$ g/mL of EpCAM protein.

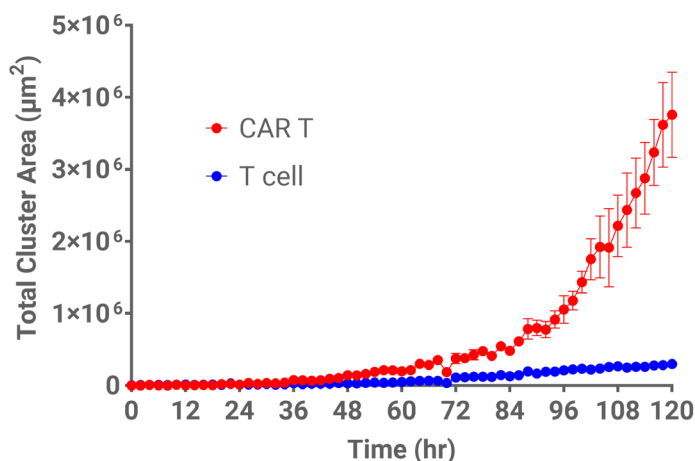


**Figure 7.** Total cluster area of CAR T and T lymphocytes treated with EpCAM. CAR T cells specific to EpCAM and untransformed T cells were exposed to 1 µg/mL EpCAM for five days and the total cluster area plotted as a function of time. Data represents the mean and standard deviation of triplicate determinations.

CAR T cell total cluster area increases steadily over time following exposure to their engineered target. CAR T lymphocytes, exposed to different concentrations of EpCAM protein exhibit cell cluster formation relative to EpCAM levels (Figure 8). CAR T cells exposed to media alone exhibit a slight increase in cluster formation comparable to nonengineered T cells in the presence of EpCAM.

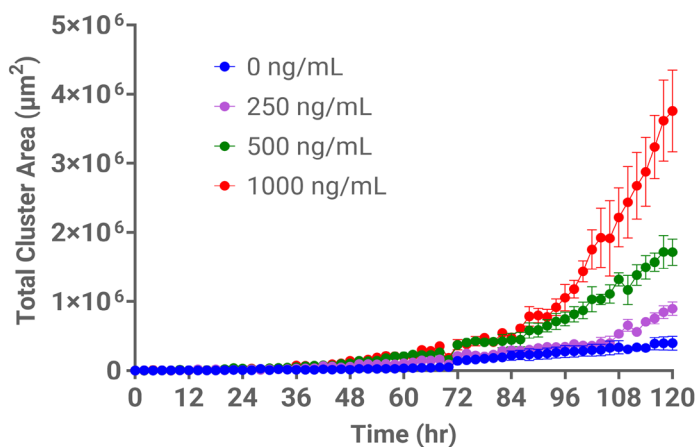


**Figure 8.** Total cluster area of CAR T cells exposed to various concentrations of EpCAM protein. CAR T cells specific towards EpCAM were exposed to various concentrations of EpCAM. Brightfield images were captured every two hours for five days. Data represents the mean and standard deviation of triplicate determinations.

Kinetic area under the curve (AUC) analysis of CAR T cells treated with a range of EpCAM concentrations demonstrates the relationship between epitope concentration and T cell cluster formation, increasing concentrations of EpCAM resulted in corresponding increases in total cluster area over time (Figure 9).

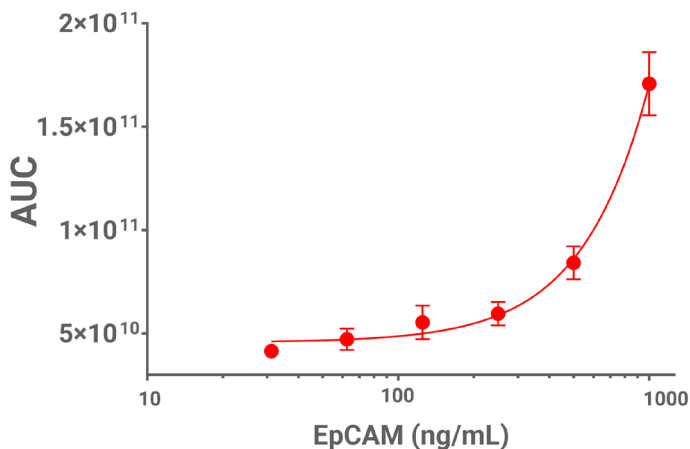


**Figure 9.** Relationship of cluster area and EpCAM concentration. CAR T cells specific towards EpCAM were exposed to various concentrations of EpCAM and brightfield images were captured every two hours for five days. Total AUC values were derived from the kinetic profiles for each EpCAM concentration tested. Data represents the mean and standard deviation of triplicate determinations.

### Quantification of CAR T cell activation in the presence of antigen-presenting target cells

CAR T cells will also form clusters in the presence of mammalian cells expressing the target surface protein. CAR T cells targeting EpCAM were cocultured with T47D-mKate cells, which express EpCAM surface protein as well as a red fluorescent nuclear marker (Figure 10). In the presence of these target cells in 2D culture, CAR T cell clusters form more rapidly compared the conditions in which the CAR T cells are exposed to EpCAM in solution.

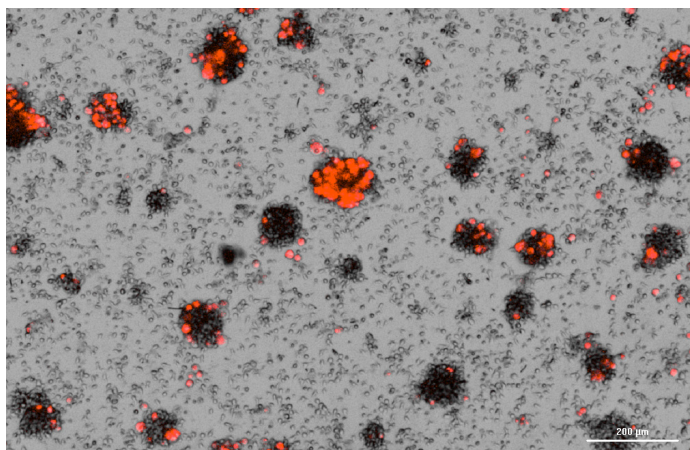


**Figure 10.** Fluorescence and brightfield image of T47D-mKate2 cells and CAR T lymphocyte clusters. Digitally zoomed 4x image of T47D-mKate cells with expressed red nuclear label incubated with a 20:1 ratio of CAR T cells to mammalian cells.

The size and quantity of the clusters can be quantitated over time. The highest concentration of CAR T cells, which reflects a 40:1 ratio of T cells to target cells, rapidly forms smaller clusters, which diminish in number over time (Figure 11). Lower effector:target (E:T) ratios form clusters at a slower pace, with some conditions exhibiting an apparent decline in cluster number. T47D-mKate2 cells not exposed to CAR T cells do not form any appreciable dark clusters.

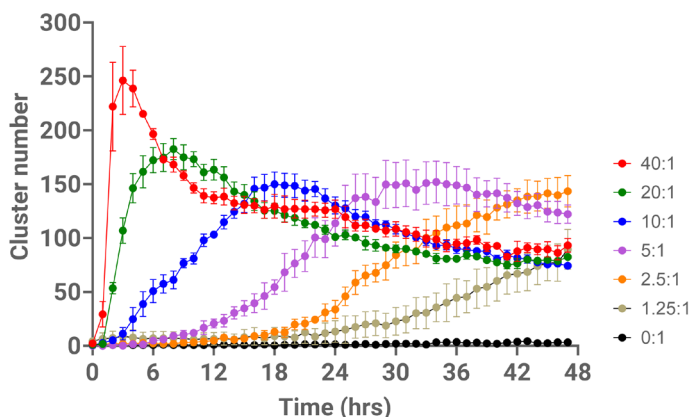


**Figure 11.** CAR T cell cluster counts from different CAR T cell to target T47D-mKate2 cell ratios. The number of CAR T cell clusters was determined at each time point for various CAR T cell to target cell ratios and plotted as a function of time.

The clusters start out as a high number of relatively small clusters, that eventually coalesce into fewer, but larger clusters. While the absolute number of clusters rapidly peaks and drops off the total cluster area rises steadily to a plateau. Total cluster area increases rapidly at high E:T ratios before reaching a steady state relatively quickly. Lower E:T ratios result in a slower onset and rate of cluster formation (Figure 12). Taken together, total cluster area was found to be the more reliable metric over cluster number.

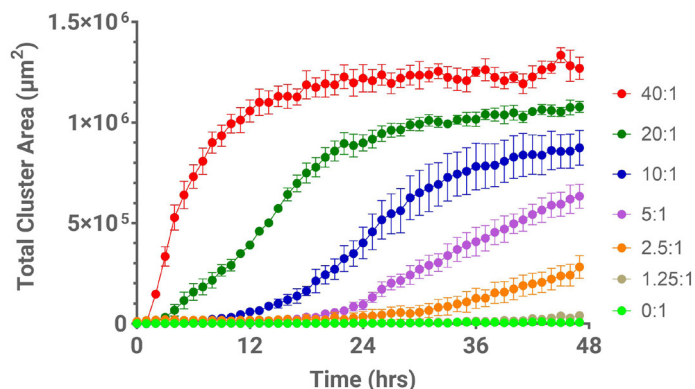


**Figure 12.** Total CAR T cell cluster area resulting from different CAR T to target cell ratios. The total cluster area was determined at each time point for different E:T ratios and plotted as function of time. Data represents the mean and standard deviation of four determinations.

## Automation

Multiplate T cell activation experiments can be performed using the Agilent BioTek BioSpa 8 automated incubator in conjunction with any Agilent BioTek Cytation cell imaging multimode reader. The Agilent BioTek BioSpa live cell analysis system can be further combined with Agilent BioTek washers and dispensers for full workflow automation of up to eight microplates. The robotic arm moves the microplate from the incubator to the imager as needed and returns it after the imaging session. The incubator system provides real-time control, continuous temperature, and CO<sub>2</sub>/O<sub>2</sub> and humidity level monitoring. The integrated BioTek BioSpa 8 provides reproducible multiplate approach for measuring T cell activation.

To evaluate the ability to expand this automated imaging-based approach for measuring T cell activation to a multiplate application, replicate plates were loaded into an integrated Cytation 5 and BioSpa system. Under assay conditions similar to those described previously, CAR T cells cultured with target T47D-mKate2 cells were monitored for cluster formation. The resulting kinetic plots of the two replicate microplates exhibit nearly identical cluster formation profiles for both positive and negative conditions, wells with and without CAR T cells, respectively (Figure 13). As expected, the corresponding kinetic AUC analysis of the total cluster area profiles forms nearly identical AUC plots (Figure 14). These results demonstrate the general reproducibility of this multiplate higher throughput system.

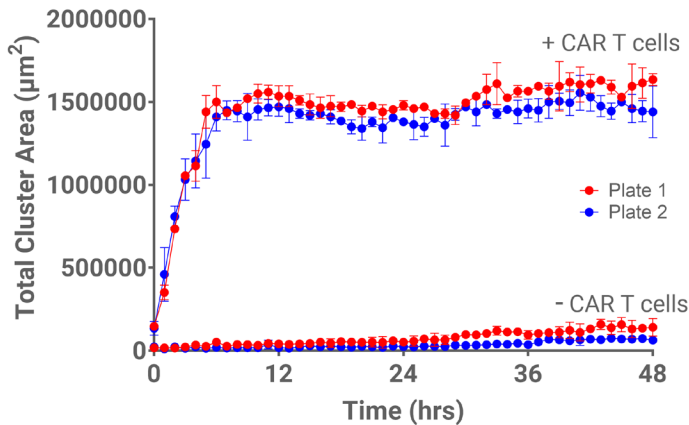


**Figure 13.** Kinetic plots of CAR T cell clusters on T47D-mKate2 cells. CAR T cells (100,000) or media only were added to T47D-mKate2 cells (5000 cells/well) in paired replicate plates (plates 1 and 2). Using an Agilent BioTek BioSpa 8 automated incubator to control incubation and plate movements, brightfield images were captured using a 4x objective every hour for 48 hours. Image analysis was used to determine total CAR T cell cluster area for each time point. Data was plotted as a function of time and represents the mean and standard deviation of duplicate samples.

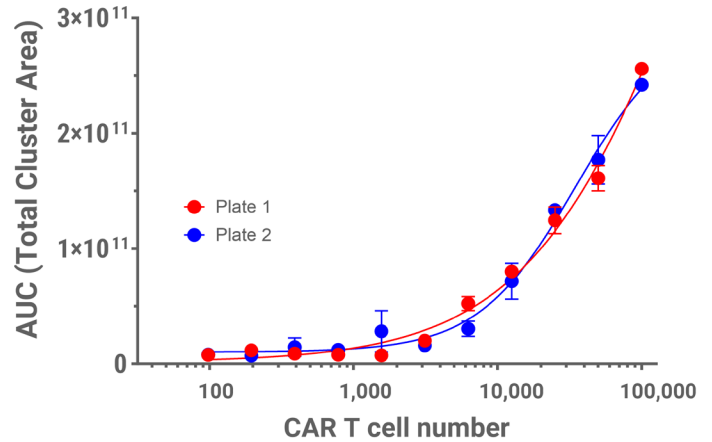


**Figure 14.** Plate-to-plate comparison of CAR T cell cluster formation. Dilutions of CAR T cells were added to T47D-mKate2 cells (5000 cells/well) in two separate plates. Using an Agilent BioTek BioSpa 8 automated incubator to control incubation and plate movements, brightfield images were captured using a 4x objective every hour for 48 hours. Image analysis was used to determine total CAR T cell cluster area for each time point. Using kinetic analysis, the subsequent AUC for each CAR T lymphocyte cell concentration was calculated and plotted as a function of cell number. Data represents the mean and standard deviation of duplicate samples.

### Demonstration of full eight-plate capacity application

Data from different cell lines and separate microplates can be used to test repeatability of the BioSpa system in a maximal capacity run. As seen in Figure 15, the plate-to-plate results from four different cell lines agree quite well. While each cell line had different degrees of cluster formation based on their cell surface antigens, the results from replicate microplates demonstrate highly similar logistic fit curves.

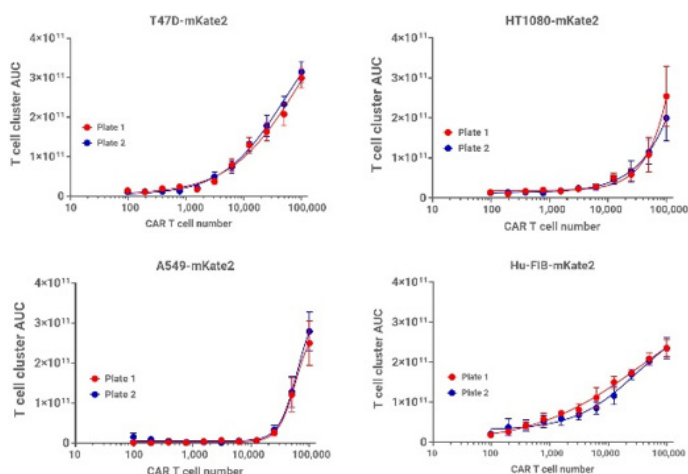


**Figure 15.** Plate-to-plate comparison of CAR T cell cluster formation with four cell lines. Dilutions of activated CAR T cells were added to two separate plates each for four cell lines: T47D-mKate2, HT1080-mKate2, A549-mKate2, and hu-FIB-mKate2 cells. Using the Agilent BioTek BioSpa 8 automated incubator to control incubation and plate movements, brightfield images were captured using a 4x objective every three hours for 48 hours. Image analysis was used to determine total CAR T cell cluster area for each timepoint. Using kinetic analysis, the subsequent AUC for each CAR T lymphocyte cell concentration is calculated and plotted as a function of cell number. Data represents the mean and standard deviation of duplicate samples.

This data indicates that this automated imaging-based assay provides a robust solution for measuring T lymphocyte activation and cluster formation. Cell number determination by brightfield microscopy is a noninvasive means to assess cell proliferation. While T cell lymphocyte IL-2-induced proliferation can be detected using image-based analysis of high content brightfield imaging, nonviable cells cannot be distinguished from actively growing cells. This can reduce the statistical significance of the measurement. Brightfield microscopy also suffers from the propensity of cells to migrate to the well edge and move out of the standard imaging region. Assays that depend on live-cell molecules such as ATP are a better option to accurately quantitate cell proliferation. While these assays are destructive in nature, cell lysis provides a more homogenous sample for determination.

Cluster formation and cluster size is dependent on the number of T cells present. With activation, T cells (both CAR T and normal lymphocytes) form dense aggregates, and can be observed with brightfield microscopy. CD3 and CD28 are proteins expressed by T cells that serve as costimulatory agents for activation and proliferation *in vivo*.<sup>3</sup> Normal T cells activated by exposure to CD3/CD28 achieve a maximal cluster area after about five days of exposure, provided a saturating amount of stimulant is present. Likewise, when CAR T cells are stimulated using their designated target (EpCAM) they form clusters in a cell number dependent manner. Normal naïve T cells are not stimulated with exposure to EpCAM, indicating that this protein is not recognized as foreign by normal TCRs. In addition to EpCAM in solution, cluster formation can also be induced by the presence of EpCAM on the surface of target cells. T47D-mKate 2 cells have been shown to express high levels of EpCAM of their surface, making it available to activate CAR T cells designed to recognize it.<sup>6</sup> Under these conditions, the target cells also provide the nucleus for cluster formation, allowing small clusters to form more rapidly than when the stimulant is in solution.

These multiday experiments use live target and T cells, requiring environmental control of temperature, humidity, and CO<sub>2</sub>. The Lionheart FX automated microscope is an ideal platform for single-plate experiments when configured with a humidity chamber and a gas controller. Multiplate assays can be automated using a BioSpa 8 automated incubator to control environmental conditions and transport the microplate to an attached imaging system.

## Conclusion

This study demonstrates the effectiveness of a label-free, imaging-based assay for monitoring T cell and CAR T cell activation through cluster formation. By leveraging brightfield microscopy and Agilent BioTek Gen5 software for imaging and microscopy, researchers can quantify immune cell responses in real time, offering a noninvasive and scalable method for evaluating activation kinetics. The assay reliably distinguishes between activated and nonactivated cells, with cluster size and formation dynamics reflecting stimulant concentration and effector:target (E:T) ratios. These findings highlight the assay's use in both basic immunology and applied therapeutic development.

Furthermore, the integration of automated systems like the Agilent BioTek BioSpa 8 automated incubator and Agilent BioTek Cytation 5 cell imaging multimode reader enables high-throughput, reproducible analysis across multiple plates and cell lines. This automation supports consistent environmental control and imaging, making it ideal for extended, live-cell experiments. The platform's flexibility and scalability position it as a valuable tool for immunotherapy research, particularly in optimizing CAR T cell design and function. Overall, this approach provides a robust framework for advancing cell-based assays in both research and development settings.

## References

1. Feinerman, O; Germain, RN; Altan-Bonnet, G. Quantitative Challenges in Understanding Ligand Discrimination by Alpha Beta T Cells. *Mol Immunol*, **2008**, 45(3), 619–631. DOI: [10.1016/j.molimm.2007.03.028](https://doi.org/10.1016/j.molimm.2007.03.028)
2. Srivastava, S. and Riddell, S.R. Engineering CAR-T Cells: Design Concepts, *Trends in Immunol.*, **2015**, 36(8):494-502. DOI: <https://doi.org/10.1016/j.it.2015.06.004>
3. Gray Parkin, K; Stephan, RP; Apilado, RG, Lill-Elghanian DA; Lee, KP; Saha, B. et al. Expression of CD28 by Bone Marrow Stromal Cells and Its Involvement in B Lymphopoiesis. *J. of Immunol.*, **2002**, 169(5): 2292–2302. DOI:[10.4049/jimmunol.169.5.2292](https://doi.org/10.4049/jimmunol.169.5.2292)
4. Ferenczi, K.; Burak, L.; Pope, M.; Krueger, J.G.; Austin, L.M. CD69, HLA-DR and the IL-2R Identify Persistently Activated T Cells in Psoriasis Vulgaris Lesional Skin: Blood and Skin: Comparisons by Flow Cytometry. *J. Autoimmun.* **2000**, 14, 63. DOI: [10.1006/jaut.1999.0343](https://doi.org/10.1006/jaut.1999.0343)
5. Jackson, A.L.; Matsumoto, H.; Janszen, M.; Maino, V.; Blidy, A.; Shye, S.; Restricted Expression of p55 Interleukin 2 Receptor (CD25) on Normal T Cells. *Clin. Immunol. Immunopathol.* **1990**, 54(1), 126-33. DOI: [10.1016/0090-1229\(90\)90012-f](https://doi.org/10.1016/0090-1229(90)90012-f)
6. Martowicz, A; Spizzo, G.; and Untergasser, G. Phenotype-Dependent Effects of EpCAM Expression on Growth and Invasion of Human Breast Cancer Cell Lines. *Cancer* **2012**, 12(501). DOI: [10.1186/1471-2407-12-501](https://doi.org/10.1186/1471-2407-12-501)

## Products used in this application

### Agilent products

Agilent BioTek Lionheart FX Automated Microscope [↗](#)

Agilent BioTek Cytation 5 Cell Imaging Multimode Reader [↗](#)

Agilent BioTek BioSpa Live Cell Analysis System [↗](#)

[www.agilent.com/lifesciences/biotek](http://www.agilent.com/lifesciences/biotek)

For Research Use Only. Not for use in diagnostics procedures.

RA250623.406

This information is subject to change without notice.

© Agilent Technologies, Inc. 2025  
Published in the USA, June 27, 2025  
5994-8424EN